SMAR 2019 – Fifth Conference on Smart Monitoring,
Assessment and Rehabilitation of Civil Structures

SMAR 2019

Flying corrosion inspection robot for corrosion monitoring of civil structures – First results

Patrick PFÄNDLER [1], Karen BODIE [1], Ueli ANGST [1], Roland SIEGWART [1]
[1] ETH Zurich, Zurich, Switzerland

Contact e-mail: patrick.pfaendler@ifb.baug.ethz.ch

ABSTRACT: A main challenge in the coming decades will be the assessment of our ageing infrastructure and their repair. Automating corrosion assessments by means of inspection robots will help to lower the costs of routine inspections. In order to apply well-proven non-destructive test methods to structures a physical contact to the surface is often essential. Establishing physical contact with a drone to the structure requires high stability and ideally full 6 degrees of freedom, force and torque tracking to be robust in the field. Here, in an interdisciplinary collaboration, such a flying robot equipped with electrochemical sensors to detect corrosion was developed. First flight tests with the electrochemical sensor on a laboratory sample demonstrate that electrochemical steel potentials and electrical concrete resistance can be successfully measured by the robot and are comparable to measurements taken conventionally.

1 INTRODUCTION

1.1 Significance of early corrosion detection on reinforced concrete structures

Most of the civil infrastructure is built with reinforced concrete (RC) and nowadays concrete is still by volume the most used material by mankind (Flatt et al. 2012). In most of the early deterioration problem of RC structures, the corrosion of reinforcement is the main problem (Fédération Internationale du Béton (fib) 2011). In the coming decades, society will increasingly face the ageing of our infrastructure, which leads to a continuous increase in need for reliable inspection to efficiently schedule maintenance works. In addition to safety concerns, the repair and maintenance of bridges, tunnels and other civil infrastructure builds in RC will cost a considerable amount of money, in most cases paid through taxes by the society, and might will reduce the availability for the end-users (e.g. bridges or tunnels for traffic repairs). A study for highway bridges in the Netherlands forecasts a rise by a factor 2 to 4 in the next 20 years for bridge repair (Polder et al. 2012). The authors of that study assume a similar situation for many countries in Europe. An evaluation of the Swiss Federal Roads Office for highway bridges states that more than 50% of the bridges already passed the age of 35 years and consequently an increase in repair and maintenance cost was observed in recent years (Cuche et al. 2016).

In the near future in these countries, the challenge will be to maintain this large stock of infrastructure with perspective to costs, availability, and safety of course. The current manner of inspection in Switzerland (and many other countries) is solely based on a routine visual inspection at a fixed interval, such as every 5 years (Vogel and Schellenberg 2012). Hence, this approach of relying on visual inspections does not take full advantage of the available non-destructive test (NDT) methods (Figure 1). It is well known that NDT can significantly improve the quality of the diagnosis of a structure's condition, as it can reveal damage processes that are not (yet)

visually apparent. As an example, in the case of a chloride triggered corrosion attack, a loss of cross-section of the reinforcement steel typically takes place years before corrosion products are transported to the outer concrete surface where they become apparent as rust stains (Angst et al. 2012). Other NDT methods such as potential mapping, electrical concrete resistivity, and polarization resistance measurements can provide information about both the extent of corroding areas within a structure and the corrosion propagation phase (Tuutti 1982) of the service life (Bertolini et al. 2003). This information will consequently lead to a more profound basis to choose the most suitable repair method as a possible way to mitigate the increase in maintenance costs. Furthermore, savings can be achieved by a more accurate localization of reinforcement suffering a severe loss in cross section.

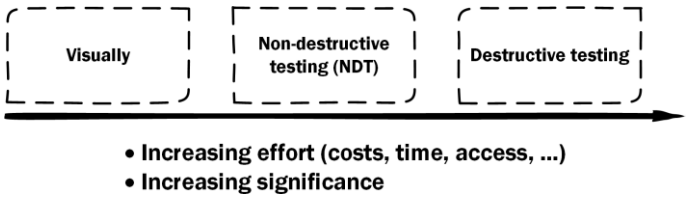

Figure 1. Importance of NDT techniques to improve condition assessments.

Today, however, the use of NDT is only taken into consideration when visual inspection indicates damage processes ongoing. For instance, potential mapping is typically performed *after* visual inspection revealed corrosion in a structure with clear signs like cracking or rust stains on the concrete surface. This technique, however, is capable of detecting chloride-induced reinforcement corrosion at an early stage, long before traces of corrosion products are visually detectable on the concrete surface (Bertolini et al. 2003). The main reasons for not using the potential mapping technique in routine inspections are due to major drawbacks in costs and limited accessibility of structural members, such as bridge underdecks. Depending on the situation, additional heavy equipment (e.g. lifting platform) is required to access parts of the object, which may require closing lanes and increases the need for personnel involved in the measurements.

1.2 Robotic inspection

The use of flying robots for inspection tasks is gaining momentum. Although, currently the unmanned aerial vehicles (UAVs) are only used for efficient visual inspection tasks due to limited interaction capabilities with the environment respectively with the parts of the structural member. A number of approaches are UAVs and climbing robots with the idea to automate the inspection task can be found in the literature (Lattanzi and Miller 2017). The main finding for applications is that almost all robots rely on image-based condition assessment with the drawbacks mentioned in the previous section. Due to this fact, several researchers already tackled the challenge to automatically detect cracks or other deterioration mechanisms on images, videos or in real time with machine vision-based (Ye et al. 2016) or with machine learning approaches. Only a limited number of attempts are made to combine visual inspection with NDT methods to increase the significance and the effectiveness of a condition assessment (Reichling et al. 2009; Kee et al. 2015). The main issue of those systems is the limitation to reach and take measurements at locations on structural members that are effortful to access, since these robots were not developed with this purpose in mind. In order to overcome this limitation and to enhance the current manner of inspection structures with robots, we propose to take full advantage of the recent developments in omnidirectional aerial vehicles, which allow physical interaction with the environment. This omnidirectional flying platform allows the use of NDT methods like potential mapping that requires physical contact to the concrete surface and an electrical connection to the reinforcing steel.

This paper presents the results of preliminary indoor flights with the flying corrosion inspection robot equipped with a saturated copper/copper-sulfate electrode (CSE) for potential mapping on a small reinforced concrete specimen with an artificially placed localized corrosion spot close to one end of the concrete block. The obtained data is presented compared to the known location of the locally corroding reinforcement from the sample preparation and in the last part of this contribution, some ideas for future research directions are proposed.

2 METHODOLOGY

2.1 Flying Robot

For physical interaction with the structure with an electrochemical sensor, a novel omnidirectional aerial system was developed by Autonomous Systems Lab (ASL) at ETH (Figure 2). The present solution is an omnidirectional hexarotor with actively tilting double propellers, which allows full exerting force and torque exertion in all directions while maintaining a fixed position in the air. The NDT sensor for physical interaction is mounted on a rigid end-effector with a length of 0.64 m. The flying robot has a weight of 4.75 kg including payload and 6 rotor groups with a maximum thrust of 10 N per motor. The diameter of the complete system without the rigid arm is 0.83 m. During the preliminary flights, the robot was secured with a safety rope from the top. The CSE was placed at the end-effector with a tethered cable to connect to the reinforcement of the concrete specimen to allow the measurements.

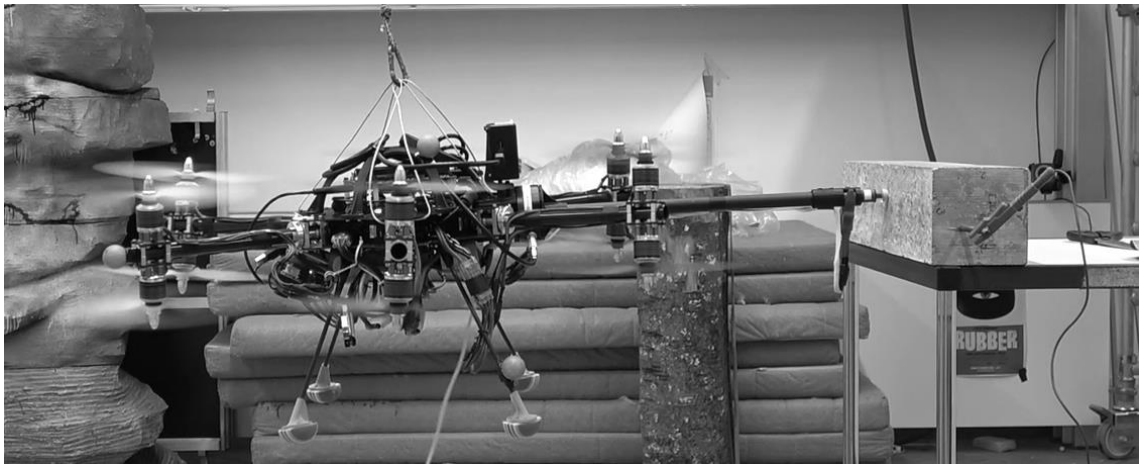

Figure 2. Flying corrosion inspection robot (hexarotor) with inclined propellers measuring electrical concrete resistances and potentials on a concrete block (side A) secured by a safety rope from the top.

2.2 Experimental program

The objective of the experimental program was to combine the electrochemical sensor with the flying robot and to validate measurements performed with the robot against measurements taken conventionally. The concrete specimen had the dimensions 500 × 100 × 100 mm and was reinforced with an eccentrically placed carbon steel bar with Ø6 mm (B500B) resulting in cover depths of 27, 37, 57 and 67 mm. Close to one end of the rebar, a mortar layer was cast around the steel containing chlorides (3.75% per mass of cement) with a length of approximately 75 mm, before the concrete beam was cast with a concrete of w/c = 0.60 and a maximum aggregate size of 16 mm. This chloride mortar was to ensure localized corrosion of the reinforcement close to one end of the beam (Vonäsch and Knuser 2013).

The probe used for the potential measurements was designed to meet requirements by the flying robot (in terms of lightweight, shape, etc.). The reference electrode was of the type CSE, which here consisted of a copper tube with (length 54 mm, and outer diameter 15 mm), filled with saturated copper sulphate solution. Through a thread on one side, a plastic head was placed. The head has a centric hole of 5 mm in diameter closed with a wooden plug to prevent leakage of the solution. The electrode has a total weight of 30 g including the solution and without the crocodile clip. The electrolytic contact with the surface was ensured with a sponge, resulting in a contacting area around 1.8 cm^2 depending on the applied contact force.

The electrochemical sensor can not only measure potentials, but also the electrical concrete resistance between the reference electrode and the embedded reinforcing steel. These parameters were measured at each spot where the robot established physical contact between probe and concrete specimen. The electrical resistance was measured by a handheld (Escort ELC 131-D) with AC current (1 kHz) and the value was manually noted. The potentials were logged with the handheld multimeter (UNI-T UT61 D, input impedance of 3000 MΩ for the mV range) with a sampling rate of 0.7 Hz for 5 s at each measured spot, thus resulting in 7 to 8 potentials per location.

The electrical concrete resistance was measured between a disc (the electrode) placed on the concrete surface and the reinforcing steel, and corrected by the inner resistance of the electrode (that was determined in separate experiments). This inner resistance of the copper sulphate electrode depends on the moisture state of the sponge. We checked the inner resistance regularly in the laboratory with an impedance measurement on a metal plate; the value was found to be 3.5 kΩ for a fully saturated sponge. The CSE was wetted with tap water before each flight to ensure good electrical contact with the pore system of the block and reliable measurements.

The flying robot navigated in total three times towards 9 points spaced every 50 mm along the sample, using pre-defined trajectories. The first flight and its repetition were done on side A with a cover of 27 mm and the third flight was done on side B with a cover of 67 mm. The flying inspection robot was directed to the middle of the height of the sample placed around 1.5 m above ground and to stay with the sensor in full contact until all data has been taken. The flights are performed with an external state estimation (vicon motion capture with 250 Hz) via gray markers distributed at selected locations on the robot, whereas the force towards the concrete block was estimated by the on-board momentum-based wrench estimator, which provides a damped estimate of the actual contact force. After the contact with the concrete surface, the robot hovered perpendicularly away from the surface, moved parallel to the specimen, and started to approach the next spot. The described procedure to move from one spot on the sample to the next took around 13 s to complete.

3 RESULTS OF THE FIRST FLIGHTS

Figure 3 shows the results of the potential and electrical concrete resistance measurements along the concrete specimen. A comparison between the shapes of the curves shows almost the same behavior. There are a potential drop and a drop in the electrical resistance compared to the surrounding points caused by the artificially generated localized corrosion of the reinforcement and the mortar with chlorides.

The graph in Figure 4 shows the potential as a function of time, measured during the 5 s after the contact of the sensor to the concrete surface was established. The data confirm for the flight on side A its repetition a stable potential reading over time tough the last data of the other side indicate some changes in the potential especially during the first second of recording of several different locations. The decrease in the potential value is might be caused by a movement of the

CSE triggered by the robot's end-effector, which was seen several times on the video. The measured potential at 25 cm from the flight on side B indicates a change of the potential in the positive direction after approx. 4 s measuring time (Figure 4 (c)), which is possibly caused by a high local electrical concrete resistance (Figure 3 (b)). Finding rather small anodes with high covers in a dry environment is generally difficult.

Figure 5 shows the estimated contact force (around 1.6 N) of the electrochemical sensor at the concrete surface. This clearly shows that the force was constant during the contact in this flight. The flat parts of the curve indicate the contact with the specimen and a wall contact time between 13 to 21 s per location on the sample.

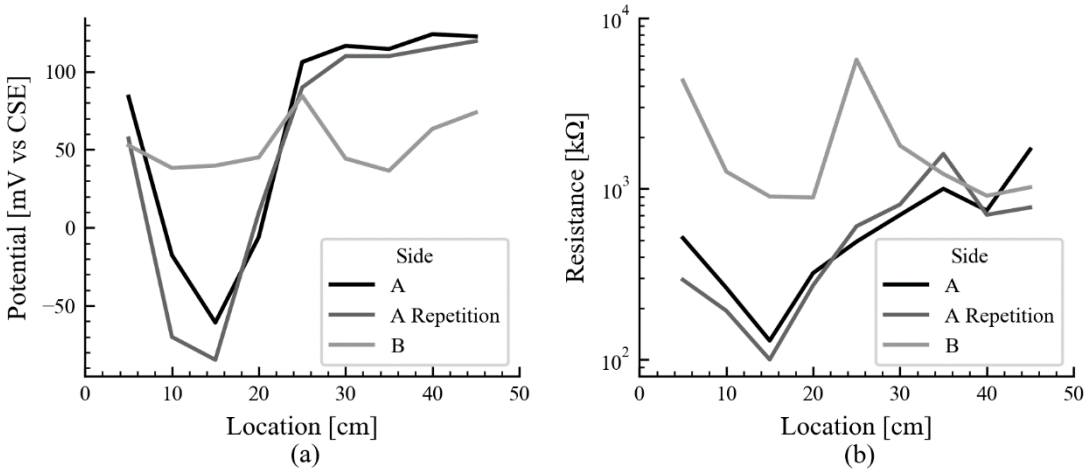

Figure 3. (a) Potential (median value of 5 s recorded potentials) against the CSE of the flights on sides A and B, and (b) Electrical concrete resistance from the CSE to the reinforcement.

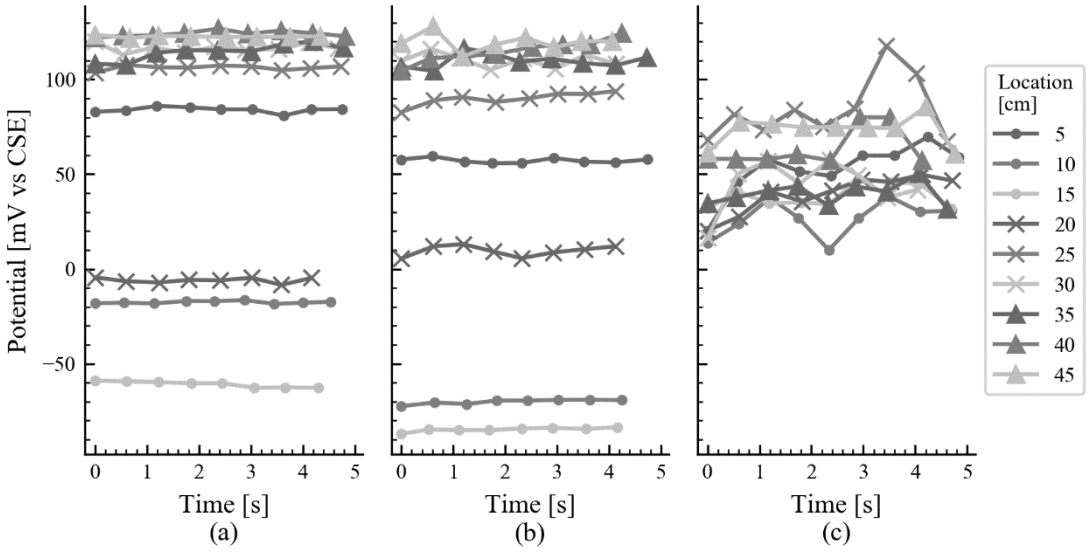

Figure 4. Recorded potentials on the sample at the 9 spots during the flights: (a) Side A, (b) Side A Repetition flight and (c) Side B.

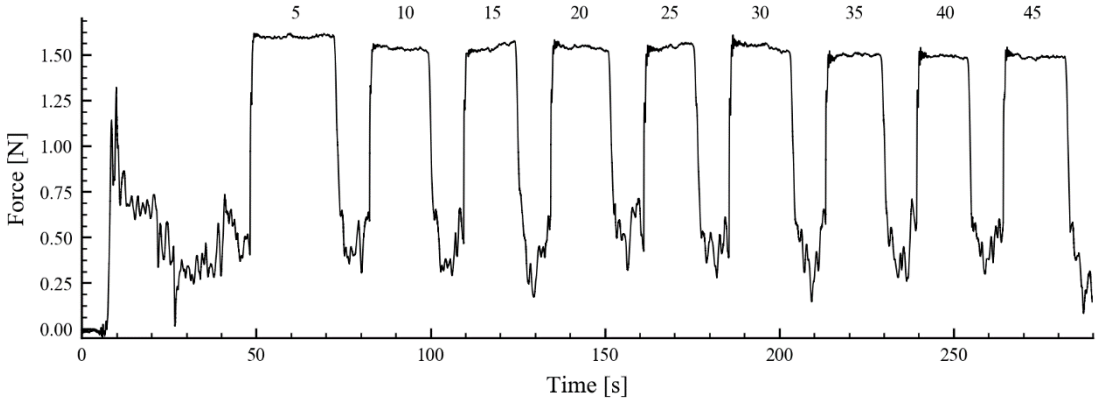

Figure 5. Force applied by the robot's end-effector to the sample during the flight on side A Repetition with a bias in the force estimator and the coordinates in centimeters.

4 DISCUSSION

A pure visual inspection of the specimen did not show any traces of rust on the concrete surface. In other words, visual inspection would in this case not allow to detect the localized corrosion ongoing in the sample. This is an obvious drawback of the visual inspection in terms of early corrosion detection.

On the other hand, considering the results of the electrochemical and electrical measurements, allows detecting the corroding site in the specimen. Figure 6 shows the results in terms of electrical concrete resistance vs. steel potential and contains information about the location of the localized corrosion spot (which is known from the sample preparation) (Elsener and Böhni 1997). As expected, the representation of the data shows for the two flights on side A, a clear separation between the areas of the reinforcing steel suffering to localized corrosion and the other parts remaining in the passive state. The performance on the evaluation of the flight on side B (higher cover depth) was not as successful as anticipated. However, the values for the potential reading are rather high compared to expected values for actively corroding steel reinforcement in dry concrete (Bertolini et al. 2003). Nonetheless, the potential drop of around 150 mV on side A is the same drop as measured during measurements taken by the conventional method half a year earlier in a comparable environment (indoor, dry) with the same electrode.

The consumed time to reach and measure one point of the specimen is currently in the order of 30 s. This is too slow for an application on a real civil engineering structure, where several thousands of points are needed to be measured to obtain a complete condition assessment. The manual reading of the resistance values from the handheld influenced the time per point as well negatively. This can be greatly improved in future developments (see 6 Outlook).

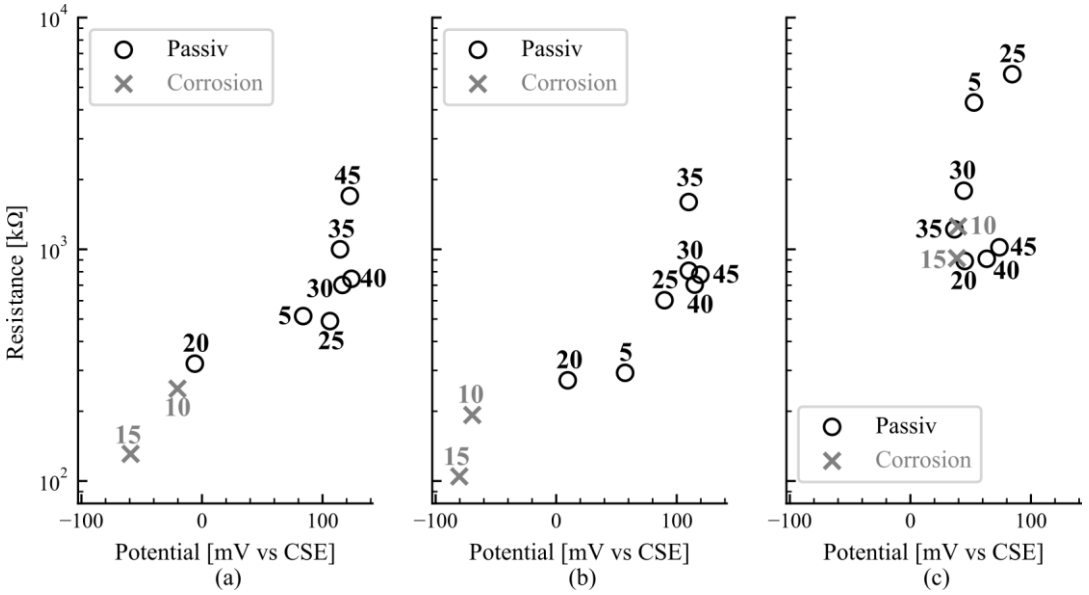

Figure 6. Combined plot of potential and resistance on the specimen with the location in centimeters on the following flights: (a) Side A (b) Side A Repetition and (c) Side B.

5 CONCLUSIONS

In summary, this paper showed successful first flights and measurements with the flying corrosion inspection robot equipped with an electrochemical sensor on a laboratory sample with a localized corrosion spot. The analysis of the acquired data is comparable to measurements taken conventionally. Our flights show that the approach of a flying robot for NDT inspection tasks, in which physical contact between sensor and concrete structure is required, is feasible. We would like to mention that the presented results are preliminary results and part of an ongoing collaborative research effort.

6 OUTLOOK

The main limitation of the flying robot includes its dependence from the external state estimation. The robot has the ability to place the electrochemical sensor on more complex geometries than the rectangular cuboid shaped concrete block. Existing techniques for on-board state estimation can overcome the reliance on external cameras, and permit inspection of outdoor infrastructure in future applications.

It will be crucial in the future to speed up the data acquiring process while maintaining the same data quality level. A point measurement currently takes 30 s, which is too slow for a complete, condition assessment of a structure. At a later stage of the project, it is expected that only one engineer is required to supervise the robot, whereas several persons supervised the robot during this preliminary flight. This improvement is going to reduce the personnel involved and consequently the inspection costs. Another solution to speed up the potential measurement will be to develop a small wheel electrode for continuous measurements (Leibbrandt et al. 2012).

The flying corrosion inspection robot was designed for condition assessments of hardly accessible parts of structural members with contact-based NDT methods. But the robotic platform opens up further possibilities for other applications, where physical contact is essential.

The payload of the robotic system is not fully exploited to leave room for other NDT methods in order to enhance the current manner of the condition assessment of RC structures. Future research efforts will examine an estimate for the resistivity of the concrete instead of the presented electrical concrete resistance. The resistivity will take advantage of this measurement because of the relationship between the resistance and the corrosion risk and even the corrosion of steel embedded in concrete (Hornbostel et al. 2013) and might reveal more information about the propagation phase of the service life model (Tuutti 1982; Bertolini et al. 2003).

7 ACKNOWLEDGEMENTS

The authors kindly acknowledge the funding of this project provided by an ETH Grant.

8 REFERENCES

Angst U, Elsener B, Jamali A, Adey B (2012) Concrete cover cracking owing to reinforcement corrosion - Theoretical considerations and practical experience. In: Materials and Corrosion. John Wiley & Sons, Ltd, pp 1069–1077

Bertolini L, Elsener B, Pedeferri P, Polder RB (2003) Corrosion of Steel in Concrete. Wiley-VCH Verlag GmbH & Co. KGaA, Weinheim, FRG

Cuche A, Gozzer D, Linder L, et al (2016) Netzzustandsbericht - Bericht der Nationalstrassen

Elsener B, Böhni H (1997) Understanding Corrosion Mechanisms of Metals in Concrete - A Key to Improving Infrastructure Durability. In: Half-cell potential measurements – From theory to condition assessment of RC structures. Cambridge

Flatt RJ, Roussel N, Cheeseman CR (2012) Concrete: An eco material that needs to be improved. Journal of the European Ceramic Society 32:2787–2798. doi: 10.1016/J.JEURCERAMSOC.2011.11.012

Hornbostel K, Larsen CK, Geiker MR (2013) Relationship between concrete resistivity and corrosion rate – A literature review. Cement and Concrete Composites 39:60–72. doi: 10.1016/j.cemconcomp.2013.03.019

in Fédération Internationale du Béton (fib) (2011) Condition control and assesment of reinforced concrete structures exposed to corrosive environments (carbonation/chlorides).

Kee S-H, Maher A, La H, et al (2015) Implementation of a Fully Autonomous Platform for Assessment of Concrete Bridge Decks RABIT. pp 367–378

Lattanzi D, Miller G (2017) Review of Robotic Infrastructure Inspection Systems. Journal of Infrastructure Systems 23:04017004. doi: 10.1061/(asce)is.1943-555x.0000353

Leibbrandt A, Caprari G, Angst UM, et al (2012) Climbing robot for corrosion monitoring of reinforced concrete structures. 2012 2nd International Conference on Applied Robotics for the Power Industry, CARPI 2012 2012–Janua:10–15. doi: 10.1109/CARPI.2012.6473365

Reichling K, Raupach M, Wiggenhauser H, et al (2009) BETOSCAN-An Instrumented Mobile Robot System for the Diagnosis of Reinforced Concrete Floors BETOSCAN-Ein mobiles Roboter Messsystem für die Diagnose von bewehrten Betonböden Zusammenfassung

Tuutti K (1982) Corrosion of steel in concrete. Lund University

Vogel T, Schellenberg K (2012) Design for inspection of concrete bridges. Materials and Corrosion 63:1102–1113. doi: 10.1002/maco.201206721

Vonäsch R, Knuser R (2013) Modellprobekörper für Potentialmessungen - Herstellung und Simulation

Ye XW, Dong CZ, Liu T (2016) A Review of Machine Vision-Based Structural Health Monitoring: Methodologies and Applications. Journal of Sensors 2016:1–10. doi: 10.1155/2016/7103039